Collisional equipartition rate for a magnetized pure electron plasma

Michael E. Glinsky,[a] Thomas M. O'Neil, and Marshall N. Rosenbluth[b]
University of California at San Diego, La Jolla, California 92093-0319

Kenji Tsuruta and Setsuo Ichimaru
Department of Physics, University of Tokyo, Bunkyo-ku, Tokyo 113, Japan

(Received 15 August 1991; accepted 6 January 1992)

The collisional equipartition rate between the parallel and perpendicular velocity components is calculated for a weakly correlated electron plasma that is immersed in a uniform magnetic field. Here, parallel and perpendicular refer to the direction of the magnetic field. The rate depends on the parameter $\bar{\kappa} = (\bar{b}/r_c)/\sqrt{2}$, where $r_c = \sqrt{T/m}/\Omega_c$ is the cyclotron radius and $\bar{b} = 2e^2/T$ is twice the distance of closest approach. For a strongly magnetized plasma (i.e., $\bar{\kappa} \gg 1$), the equipartition rate is exponentially small ($\nu \sim \exp[-5(3\pi\bar{\kappa})^{2/5}/6]$). For a weakly magnetized plasma (i.e., $\bar{\kappa} \ll 1$), the rate is the same as for an unmagnetized plasma except that $r_c/\bar{b}$ replaces $\lambda_D/\bar{b}$ in the Coulomb logarithm. (It is assumed here that $r_c < \lambda_D$; for $r_c > \lambda_D$, the plasma is effectively unmagnetized.) This paper contains a numerical treatment that spans the intermediate regime $\bar{\kappa} \sim 1$, and connects onto asymptotic results in the two limits $\bar{\kappa} \ll 1$ and $\bar{\kappa} \gg 1$. Also, an improved asymptotic expression for the rate in the high-field limit is derived. The present theoretical results are in good agreement with recent measurements of the equipartition rate over eight decades in $\bar{\kappa}$ and four decades in the scaled rate $\nu/n\bar{v}\bar{b}^2$, where n is the electron density and $\bar{v} = \sqrt{2T/m}$.

I. INTRODUCTION

We consider a weakly correlated pure electron plasma that is immersed in a uniform magnetic field **B**, and is characterized by an anisotropic velocity distribution ($T_\parallel \neq T_\perp$). Here, parallel ($\parallel$) and perpendicular ($\perp$) are referring to the direction of the magnetic field. We calculate the collisional equipartition rate between the parallel and perpendicular velocity components, paying particular attention to the dependence on magnetic field strength. Formally, the rate, ν, is defined through the relation $dT_\perp/dt = \nu(T_\parallel - T_\perp)$, where $dT_\perp/dt$ is interpreted as the rate of change of the mean perpendicular kinetic energy and $(T_\parallel - T_\perp)$ is assumed to be small. In general this latter assumption is necessary for $dT_\perp/dt$ to be linear in $(T_\parallel - T_\perp)$.

The equipartition rate does not depend on the magnetic field strength when the characteristic cyclotron radius $r_c = \sqrt{T/m}/\Omega_c$ is large compared to the Debye length $\lambda_D = (T/4\pi ne^2)^{1/2}$; for this case a particle orbit is nearly a straight line over the range of the shielded interaction. Here, $\Omega_c = eB/mc$ is the cyclotron frequency, n is the electron density, and we have set $T = T_\parallel \simeq T_\perp$. Since our purpose is to investigate the influence of the magnetic field on the rate, we consider only the opposite case ($r_c < \lambda_D$). For this case, the rate can be written as

$$\nu = n\bar{v}\bar{b}^2 I(\bar{\kappa}), \tag{1}$$

where $\bar{v} = \sqrt{T/\mu}$ is the thermal spread for the distribution of relative velocities, $\bar{b} = 2e^2/T$ is twice the classical distance of closest approach, and $\bar{\kappa} = \Omega_c\bar{b}/\bar{v} = (\bar{b}/r_c)/\sqrt{2}$ is a measure of magnetic field strength. In these definitions, $\mu = m/2$ is the reduced mass, and the odd factors of 2 are introduced to match notation used previously.[1] The combination of factors $n\bar{v}\bar{b}^2$ is very nearly the equipartition rate for an unmagnetized plasma[2] [i.e., $\nu = (\sqrt{2\pi}/15)n\bar{v}\bar{b}^2 \ln(\lambda_D/\bar{b})$], and the function $I(\bar{\kappa})$ accounts for all dependence on magnetic field strength.

Previous theory[1-3] has provided asymptotic expressions for $I(\bar{\kappa})$ in the two limits $\bar{\kappa} \gg 1$ and $\bar{\kappa} \ll 1$. We say that the plasma is strongly magnetized when $\bar{\kappa} \gg 1$; in this limit, the collisional dynamics is constrained by a many-electron adiabatic invariant (the total cyclotron action, $J = \Sigma_j m v_{\perp j}^2/2\Omega_c$), and the equipartition rate is exponentially small (i.e., $I(\bar{\kappa}) \sim \exp[-5(3\pi\bar{\kappa})^{2/5}/6]$).[1] We say that the plasma is weakly magnetized when $\bar{\kappa} \ll 1$; in this limit, the equipartition rate is the same as for an unmagnetized plasma,[2] except that r_c replaces λ_D in the Coulomb logarithm[3] [i.e., $\ln(\lambda_D/\bar{b}) \to \ln(r_c/\bar{b})$]. In our notation, this implies that $I(\bar{\kappa}) \sim \ln(\bar{\kappa})$.

This paper contains a numerical calculation that spans the intermediate regime $\bar{\kappa} \sim 1$ and matches onto asymptotic formulas in the two limits $\bar{\kappa} \gg 1$ and $\bar{\kappa} \ll 1$. In Sec. II, a Boltzmann-like collision operator is used to obtain an integral expression for the rate. This reduces the problem of calculating the rate to the problem of calculating $\Delta E_\perp$, the change in the perpendicular kinetic energy that occurs during an isolated binary collision. In general, an analytic expression for $\Delta E_\perp$ cannot be obtained. In Sec. III, numerical solutions for

[a] Present address: Lawrence Livermore National Laboratory, Livermore, California 94550.
[b] Also at General Atomics, La Jolla, California 92138.

 0899-8221/92/051156-11$04.00

$\Delta E_\perp$ are obtained for many initial conditions chosen at random, and the integral expression is evaluated by Monte Carlo techniques.

The paper also contains a new analytic result. In Sec. IV, we derive an improved asymptotic formula for the rate in the large field limit $\bar{\kappa} \gg 1$. A solution for $\Delta E_\perp$ is obtained as an asymptotic expansion and is then substituted into the integral expression for the rate. After substantial algebra and some numerical integrations one obtains the large $\bar{\kappa}$ asymptotic result

$$I(\bar{\kappa}) \cong \exp[-5(3\pi\bar{\kappa})^{2/5}/6]\{(1.83)\bar{\kappa}^{-7/15} + (20.9)\bar{\kappa}^{-11/15} + (0.347)\bar{\kappa}^{-13/15} + (87.8)\bar{\kappa}^{-15/15} + (6.68)\bar{\kappa}^{-17/15} + O(\bar{\kappa}^{-19/15})\}. \quad (2)$$

The exponential is the same as was obtained previously,[1] but the algebraic factor in curly brackets is different and is more accurate. Note that the second and fourth terms enter with surprisingly large numerical coefficients; it is necessary to retain these higher-order terms to obtain good agreement with the numerical results. Figure 2 in Sec. III shows a comparison of both the new asymptotic formula and the previous asymptotic formula to the numerical results.

In recent experiments[4] with magnetically confined plasmas, the equipartition rate was measured over a wide range in magnetic field strength and temperature, corresponding to a range of $\bar{\kappa}$ values from $\bar{\kappa} \cong 10^{-2}$ to 10^2. Our theoretical results agree with the experimental results to within the estimated experimental error over this whole range of $\bar{\kappa}$. In fact, it was the existence of the experimental results for intermediate field strength $\bar{\kappa} \sim 1$ that motivated the theory. In addition, a previous experiment[5] measured the equipartition rate over a range of $\bar{\kappa}$ values from $\bar{\kappa} \simeq 10^{-6}$ to 3×10^{-5}. An extrapolation of the numerical results based on the theory of Ref. 3 agrees well with these additional experimental results. Figure 3 in Sec. III shows a comparison of our theoretical results to experimental measurement over eight decades in $\bar{\kappa}$ (i.e., $\bar{\kappa} = 10^{-6}$ to 10^2).

II. INTEGRAL EXPRESSION FOR THE EQUIPARTITION RATE

In this section, a Boltzmann-like collision operator[1,6] is used to obtain an integral expression for the equipartition rate. The reader may be surprised at the use of such an operator for a problem in plasma kinetic theory, since the operator does not include the effect of Debye shielding.[7] However, the magnetic field produces a kind of dynamical shielding on a length scale that is shorter than the Debye length, so it is not a problem that the Boltzmann operator omits Debye shielding.

The dynamical screening is a consequence of the adiabatic invariant discussed in Ref. 1. For a collision in which $\Omega_c \tau \gg 1$, where τ is the duration of the collision, the perpendicular kinetic energy changes by an exponentially small amount [i.e., $\Delta E_\perp \sim \exp(-\Omega_c \tau)$]. The time τ is of order $\tau \sim r_m/v$, where $r_m = \min|\mathbf{r}_1 - \mathbf{r}_2|$ is the minimum separation between the two electrons during the collision and v is a characteristic relative velocity. Thus, the quantity $\Omega_c \tau \sim \Omega_c r_m/v$ is large and the dynamical shielding is active when $r_m > r_c = \sqrt{T/m}/\Omega_c$. On energetic grounds two electrons cannot get much closer than $\bar{b} = 2e^2/T$; so the dynamical shielding is active for all collisions in a plasma with $\bar{\kappa} \gg 1$ (i.e., $\bar{b} \gg r_c$). This is the reason that the equipartition rate is exponentially small for such a plasma. Also, one can see that the most effective collisions in producing equipartition for such a plasma are close collisions (i.e., $r_m \cong \bar{b}$). Now let us turn our attention to the regime where $\bar{\kappa} < 1$ (i.e., $r_c > \bar{b}$). Here, there are some collisions where the dynamical shielding is not active (and $\Delta E_\perp$ is large), but for all collisions with $r_m > r_c$ the shielding is active. Consequently, these latter collisions have negligible effect. Both $\bar{b}$ and r_c are assumed here to be small compared to λ_D ($\bar{b} \ll \lambda_D$ for a weakly correlated plasma and $r_c < \lambda_D$ by hypothesis); so Debye shielding plays a negligible role.

Another way to look at this is to realize that the Rostoker collision operator[8] (the analog of the Lenard–Belescu operator[9] for a magnetized plasma) provides a correct description for the large impact parameter collisions where Debye shielding is most important. Debye shielding enters this equation through the plasma dielectric function. By using the fact that $r_c \ll \lambda_D$, one can argue that the dielectric function is unity with a correction of order $(r_c/\lambda_D)^2$. We replace the dielectric function with unity in our analysis and thereby neglect the small effect of Debye shielding.

The Boltzmann-like operator can be written as

$$\frac{\partial f}{\partial t}(\mathbf{v}_1,t) = \int_0^\infty 2\pi\rho\, d\rho \int d\mathbf{v}_2 |\hat{z}\cdot(\mathbf{v}_2 - \mathbf{v}_1) \times [f(\mathbf{v}_1')f(\mathbf{v}_2') - f(\mathbf{v}_1)f(\mathbf{v}_2)], \quad (3)$$

where $f(\mathbf{v},t)$ is the electron velocity distribution and $\hat{z}$ is the direction of the magnetic field.[1] To understand the notation used, it is useful to imagine that a coordinate system is established on electron 1 and that planes are defined at $z = \pm l$, where l is much larger than the maximum of $\bar{b}$ and r_c. A collision is considered to begin when electron 2 passes into the region between the planes and to end when it passes out of the region. In the usual manner, the velocities $(\mathbf{v}_1',\mathbf{v}_2')$ evolve into $(\mathbf{v}_1,\mathbf{v}_2)$ during a collision. The quantity $\rho = |\hat{z} \times (\mathbf{r}_2 - \mathbf{r}_1)|$ is the transverse separation between the electrons at the beginning of a collision; one can think of ρ as a kind of impact parameter and of $\int 2\pi\rho\, d\rho$ as an integral over the impact parameter (or scattering cross section). The factor $|\hat{z}\cdot(\mathbf{v}_1 - \mathbf{v}_2)|$ is necessary to give the flux of electrons 2 incident on either one of the planes. Because of the magnetic field, electron 2 can interact with electron 1 only by first passing through one of the planes. Also, the dynamical shielding will provide a natural cutoff on the integral over ρ.

The rate of change of the mean perpendicular kinetic energy is given by

$$\frac{dT_\perp}{dt} = \int d\mathbf{v}_1 \frac{m v_{1\perp}^2}{2} \frac{\partial f}{\partial t}(\mathbf{v}_1,t). \quad (4)$$

Using Eq. (3) to evaluate $\partial f/\partial t$ yields the expression

$$\frac{dT_\perp}{dt} = n \int_0^\infty 2\pi\rho\, d\rho \int d\mathbf{v}_1 \int d\mathbf{v}_2 \frac{m v_{1\perp}^2}{2} |\hat{z}\cdot(\mathbf{v}_2 - \mathbf{v}_1)| \times [f(\mathbf{v}_1')f(\mathbf{v}_2') - f(\mathbf{v}_1)f(\mathbf{v}_2)], \quad (5)$$

where the distributions in the brackets are assumed to be of the form

$$f(\mathbf{v}) = \left(\frac{m}{2\pi T_\parallel}\right)^{1/2}\left(\frac{m}{2\pi T_\perp}\right)\exp\left(-\frac{mv_\parallel^2}{2T_\parallel}-\frac{mv_\perp^2}{2T_\perp}\right). \tag{6}$$

By using detailed balance, Eq. (5) can be rewritten as

$$\frac{dT_\perp}{dt} = \frac{n}{4}\int_0^\infty 2\pi\rho\, d\rho \int d\mathbf{v}_1 \int d\mathbf{v}_2\,(\Delta E_\perp)|\hat{z}\cdot(\mathbf{v}_2-\mathbf{v}_1)| \times[f(\mathbf{v}_1')f(\mathbf{v}_2') - f(\mathbf{v}_1)f(\mathbf{v}_2)], \tag{7}$$

where

$$\Delta E_\perp = \frac{mv_{1\perp}^2}{2}+\frac{mv_{2\perp}^2}{2}-\frac{mv_{1\perp}'^2}{2}-\frac{mv_{2\perp}'^2}{2} \tag{8}$$

is the change in the perpendicular kinetic energy that occurs during a collision.

It is useful to change variables from $(\mathbf{v}_1,\mathbf{v}_2)$ to $(\mathbf{V},\mathbf{v})$, where $\mathbf{V}=(\mathbf{v}_1+\mathbf{v}_2)/2$ is the center of mass velocity and $\mathbf{v}=(\mathbf{v}_2-\mathbf{v}_1)$ is the relative velocity. First let us note that the binary dynamics separates under this change of variables. The equations of motion for the two interacting electrons are

$$\frac{d\mathbf{v}_1}{dt}+\Omega_c\mathbf{v}_1\times\hat{z} = \frac{e^2}{m}\frac{(\mathbf{r}_1-\mathbf{r}_2)}{|\mathbf{r}_1-\mathbf{r}_2|^3}, \tag{9}$$

$$\frac{d\mathbf{v}_2}{dt}+\Omega_c\mathbf{v}_2\times\hat{z} = \frac{e^2}{m}\frac{(\mathbf{r}_2-\mathbf{r}_1)}{|\mathbf{r}_1-\mathbf{r}_2|^3}. \tag{10}$$

By adding and subtracting these two equations, we obtain separate equations for the center of mass motion and for the relative motion,

$$\frac{d\mathbf{V}}{dt}+\Omega_c\mathbf{V}\times\hat{z}=0, \tag{11}$$

$$\frac{d\mathbf{v}}{dt}+\Omega_c\mathbf{v}\times\hat{z} = \frac{e^2}{\mu}\frac{\mathbf{r}}{|\mathbf{r}|^3}. \tag{12}$$

Here, $\mathbf{r}=\mathbf{r}_2-\mathbf{r}_1$ is the relative position vector and $\mu=m/2$ is the reduced mass. The center of mass motion is simply motion in a uniform $\mathbf{B}$ field, so it follows trivially that $|\mathbf{V}_\perp'|=|\mathbf{V}_\perp|$ and $|\mathbf{V}_z'|=|\mathbf{V}_z|$. The solution for the relative motion is not trivial, but conservation of energy guarantees that $\mu v'^2/2=\mu v^2/2$. From these relations and the relations

$$E_\perp \equiv \frac{mv_{1\perp}^2}{2}+\frac{mv_{2\perp}^2}{2}=\frac{\mu v_\perp^2}{2}+\frac{2mV_\perp^2}{2}, \tag{13a}$$

$$E_\parallel \equiv \frac{mv_{1\parallel}^2}{2}+\frac{mv_{2\parallel}^2}{2}=\frac{\mu v_\parallel^2}{2}+\frac{2mV_\parallel^2}{2}, \tag{13b}$$

it follows that

$$\Delta E_\perp = -\Delta E_\parallel = \Delta(\mu v_\perp^2/2). \tag{14}$$

By carrying out the change of variables and by using the relation $d\mathbf{v}_1\,d\mathbf{v}_2 = d\mathbf{V}d\mathbf{v}$ as well as Eqs. (13) and (14), Eq. (7) can be rewritten in the form

$$\frac{dT_\perp}{dt} = \frac{n}{4}\int_0^\infty 2\pi\rho\, d\rho\int d\mathbf{v}|v_\parallel|\Delta\left(\frac{\mu v_\perp^2}{2}\right)f_r(v_\parallel,v_\perp) \times\left\{\exp\left[\left(\frac{1}{T_\perp}-\frac{1}{T_\parallel}\right)\Delta\left(\frac{\mu v_\perp^2}{2}\right)\right]-1\right\}, \tag{15}$$

where the integral over $d\mathbf{V}$ has been carried out and

$$f_r(v_\parallel,v_\perp) = \left(\frac{\mu}{2\pi T_\parallel}\right)^{1/2}\left(\frac{\mu}{2\pi T_\perp}\right)\exp\left(-\frac{\mu v_\parallel^2}{2T_\parallel}-\frac{\mu v_\perp^2}{2T_\perp}\right) \tag{16}$$

is the distribution of relative velocities. Finally, to first order in the small quantity $(T_\parallel - T_\perp)$ we obtain the rate equation $dT_\perp/dt = \nu(T_\parallel - T_\perp)$, where the rate ν is given by the integral expression

$$\nu = \frac{n}{4T_\parallel T_\perp}\int_0^\infty 2\pi\rho\, d\rho\int d\mathbf{v}|v_\parallel|\left[\Delta\left(\frac{\mu v_\perp^2}{2}\right)\right]^2 \times f_r(v_\parallel,v_\perp). \tag{17}$$

In this expression, one may set $T_\perp \approx T_\parallel = T$.

III. NUMERICAL CALCULATION OF THE EQUIPARTITION RATE

Equation (17) reduces the problem of calculating the equipartition rate to the problem of solving Eq. (12) for $\Delta(\mu v_\perp^2/2)$. In general this equation has only two constants of the motion, the energy, and the canonical angular momentum, so an analytic solution is not possible. In this section, Eq. (12) is solved numerically for many initial conditions chosen at random, and the integral in Eq. (17) is evaluated by Monte Carlo techniques.

In terms of the scaled variables

$$\mathbf{u}=\mathbf{v}/\bar{v},\quad \boldsymbol{\eta}=\mathbf{r}/\bar{b},\quad s=t(\bar{v}/\bar{b}), \tag{18}$$

Eq. (12) takes the form

$$\frac{d\mathbf{u}}{ds}+\bar{\kappa}\mathbf{u}\times\hat{z} = \frac{1}{2}\frac{\boldsymbol{\eta}}{|\boldsymbol{\eta}|^3}, \tag{19}$$

where $\mathbf{u}=d\boldsymbol{\eta}/ds$, and Eq. (17) takes the form $\nu = n\bar{b}^2\bar{v}I(\bar{\kappa})$, where

$$I(\bar{\kappa}) = \frac{\pi}{2}\int_0^\infty \eta_\perp\, d\eta_\perp\int_0^\infty u_\perp\, du_\perp\int_{-\infty}^{+\infty} du_\parallel\int_0^{2\pi} d\psi \times\frac{e^{-u^2/2}}{(2\pi)^{3/2}}|u_\parallel|\left[\Delta\left(\frac{u_\perp^2}{2}\right)\right]^2. \tag{20}$$

We evaluate this integral with two completely separate Monte Carlo calculations.

The first of these introduces an arbitrary weighting function $W(u_\parallel,u_\perp,\psi,\eta_\perp)$ which is used to define the transformation[10,11]

$$(u_\parallel,u_\perp,\psi,\eta_\perp)\rightarrow(x_1,x_2,x_3,x_4),$$

where

$$x_1 = \frac{1}{A_1}\int_0^{u_\parallel} du_\parallel\int_0^\infty d\eta_\perp\int_0^\infty du_\perp\int_0^{2\pi} d\psi \times W(u_\parallel,u_\perp,\psi,\eta_\perp), \tag{21a}$$

$$x_2 = \frac{1}{A_2}\int_0^{\eta_\perp} d\eta_\perp\int_0^\infty du_1\int_0^{2\pi} d\psi W(u_\parallel,u_\perp,\psi,\eta_\perp), \tag{21b}$$

$$x_3 = \frac{1}{A_3}\int_0^{u_\perp} du_\perp\int_0^{2\pi} d\psi\, W(u_\parallel,u_\perp,\psi,\eta_\perp), \tag{21c}$$

$$x_4 = \frac{1}{A_4}\int_0^{\psi} d\psi\, W(u_\parallel,u_\perp,\psi,\eta_\perp), \tag{21d}$$

and

$$A_1 = \int_0^{\infty} du_\parallel \int_0^{\infty} d\eta_\perp \int_0^{\infty} du_\perp \int_0^{2\pi} d\psi W(u_\parallel,u_\perp,\psi,\eta_\perp), \tag{22a}$$

$$A_2(u_\parallel) = \int_0^{\infty} d\eta_\perp \int_0^{\infty} du_\perp \int_0^{2\pi} d\psi W(u_\parallel,u_\perp,\psi,\eta_\perp), \tag{22b}$$

$$A_3(u_\parallel,\eta_\perp) = \int_0^{\infty} du_\perp \int_0^{2\pi} d\psi\, W(u_\parallel,u_\perp,\psi,\eta_\perp), \tag{22c}$$

$$A_4(u_\parallel,\eta_\perp,u_\perp) = \int_0^{2\pi} d\psi\, W(u_\parallel,u_\perp,\psi,\eta_\perp). \tag{22d}$$

One can easily show that the Jacobian for this transformation is given by

$$\frac{\partial(x_1,x_2,x_3,x_4)}{\partial(u_\parallel,u_\perp,\psi,\eta_\perp)} = \frac{W(u_\parallel,u_\perp,\psi,\eta_\perp)}{A_1}, \tag{23}$$

so Eq. (20) takes the form

$$I(\bar{\kappa}) = \frac{A_1}{2^{3/2}\sqrt{\pi}} \int_0^1 dx_1 \int_0^1 dx_2 \int_0^1 dx_3 \int_0^1 dx_4 \times \frac{u_\parallel u_\perp \eta_\perp e^{-u^2/2}}{W(u_\parallel,u_\perp,\psi,\eta_\perp)} \left[\Delta\left(\frac{u_\perp^2}{2}\right)\right]^2. \tag{24}$$

If we choose

$$W \sim u_\parallel u_\perp \eta_\perp e^{-u^2/2}[\Delta(u_\perp^2/2)]^2, \tag{25}$$

the integrand in Eq. (24) is reasonably uniform over the whole domain of integration, and an efficient Monte Carlo evaluation of the integral can then be obtained by choosing N sample points $p_i = (x_1,x_2,x_3,x_4)_i$ at random in the domain of integration. The value of the integral is given by

$$I(\bar{\kappa}) \approx \frac{A_1}{2^{3/2}\sqrt{\pi}} \frac{1}{N} \sum_{i=1}^{N} \left(\frac{u_\parallel u_\perp \eta_\perp e^{-u^2/2}[\Delta(u_\perp^2/2)]^2}{W(u_\parallel,u_\perp,\psi,\eta_\perp)} \right)_i, \tag{26}$$

where N is large enough that the average has converged, that is, that fluctuations in the average as N is increased are negligible.

The choice for W requires some knowledge of $\Delta(u_\perp^2/2)$, but this knowledge need not be detailed. A good choice for W is one that captures the main features of expression (25) but is still simple enough that the integrals in transformation (21) can be carried out analytically. This provides for a reasonably rapid convergence and an efficient algorithm for choosing sample points. For the parameter regime $\bar{\kappa} > 1$, we use an expression for $\Delta(u_\perp^2/2)$ that is based on the large $\bar{\kappa}$ asymptotic analysis of Sec. IV, and for the parameter regime $\bar{\kappa} < 1$ we use an expression for $\Delta(u_\perp^2/2)$ that is based on integration along unperturbed orbits.

For a given set of random numbers $(x_1,x_2,x_3,x_4)_i$ the corresponding variables $(u_\parallel,u_\perp,\eta_\perp,\psi)_i$ specify the state of an incident electron when it first crosses one of the two planes at $\eta_\parallel = \pm l/\bar{b}$. Starting from this initial condition, orbit equation (19) is integrated forward using a Bulisch–Stoer algorithm[11] until the electron again crosses one of the two planes, and $\Delta(u_\perp^2/2)$ is calculated. The distance l must be chosen to be large enough that a further increase in l does not significantly change the numerical result for the rate. Over most of the range in $\bar{\kappa}$, this simply means that l must be many times larger than the maximum of $\bar{b}$ and r_c. However, the orbit integration is particularly time consuming in the limit of large $\bar{\kappa}$; the cyclotron frequency is much larger than the frequency characterizing the duration of a collision, and the quantity to be calculated, $\Delta(u_\perp^2/2)$, is exponentially small. Consequently, special care must be taken in this limit. The adiabatic invariant is given by an asymptotic series, the first term of which is $u_\perp^2$.[12] The higher-order terms are all zero at $\eta_\parallel = \pm\infty$, so $\Delta u_\perp^2$ is the change in the invariant when $\eta_\parallel$ varies from $+\infty$ to $-\infty$. However, at $\eta_\parallel = \pm l/\bar{b}$, the higher-order terms are not zero. We assume that the adiabatic invariant (full asymptotic series) does not change significantly when $\eta_\parallel$ varies from $+\infty$ to $l/\bar{b}$ and then again when $\eta_\parallel$ varies from $-l/\bar{b}$ to $-\infty$. The change in $u_\perp^2$ as $\eta_\parallel$ varies from $+\infty$ to $-\infty$ (i.e., $\Delta u_\perp^2$) is then given by the change in the adiabatic invariant (full asymptotic series) as $\eta_\parallel$ varies from $l/\bar{b}$ to $-l/\bar{b}$. This latter quantity must be calculated numerically. In practice, only one higher-order term is necessary to give the required accuracy.

Also, the value of $u_\parallel$ at $\eta_\parallel = l/\bar{b}$ must be related to the value of $u_\parallel$ at $\eta_\parallel = \infty$. Here, one can approximate $u_\perp^2$ as constant and use conservation of energy to write

$$u_\parallel^2(\infty) - u_\parallel^2(l/\bar{b}) \approx 2/\sqrt{\eta_\perp^2 + (l/\bar{b})^2}. \tag{27}$$

This correction becomes important at large values of $\bar{\kappa}$ because $\Delta(u_\perp^2/2)$ depends exponentially on $u_\parallel(\infty)$. The Monte Carlo calculated values of $I(\bar{\kappa})$ were found to be independent of reasonable changes in both the functional form of W and the parameters used in the integration of Eq. (19) (e.g., accuracy of the integration and the location of the plane at $l/\bar{b}$).

The integral expression for the rate was evaluated independently with a second Monte Carlo method. In this method a sample point is chosen by the rejection method,[11] which allows the treatment of more realistic and complicated weighting functions, but is somewhat slower (particularly when the weighting function is peaked). Also, the orbit equation is solved with a fourth-order Runge–Kutta algorithm.[11] The results for the two methods are the same to within expected statistical error for the $\bar{\kappa}$ values where both methods were applied.

Table I lists values for $I(\bar{\kappa})$ obtained with the integral transform method for $\bar{\kappa}$ values ranging from 10^{-4} to 10^4. The values of $I(\bar{\kappa})$ obtained by use of the rejection method are shown in Table II. These data cover $\bar{\kappa}$ values from 10^0 to 10^3. In Fig. 1 both sets of data are plotted versus $\bar{\kappa}$ and are compared to asymptotic formulas for $\bar{\kappa} \gg 1$ and $\bar{\kappa} \ll 1$. The solid curve is the large $\bar{\kappa}$ asymptotic formula given in Eq. (2), and the dashed curve is the small $\bar{\kappa}$ formula $-(\sqrt{2\pi}/15)\ln(C\bar{\kappa})$.[3] Here, C is a constant which we determine numerically to be $C = 0.333(65)$.

Some words of explanation concerning the logarithmic dependence for small $\bar{\kappa}$ and our determination of the constant $C = 0.333(65)$ may be useful. First let us review how the logarithmic dependence comes about. For collisions characterized by $\bar{b} < r_m < r_c$, where $r_m = \min|\mathbf{r}_1 - \mathbf{r}_2|$ is the

TABLE I. Results of Monte Carlo calculation using the integral transform method. Statistical error in the last two significant figures is shown in parentheses.

$\bar{\kappa}$	$I(\bar{\kappa})$
1.00×10^{-4}	$1.753(63)\times10^{0}$
1.00×10^{-3}	$1.335(44)\times10^{0}$
1.00×10^{-2}	$9.26(45)\times10^{-1}$
1.00×10^{-1}	$5.90(36)\times10^{-1}$
3.33×10^{-1}	$3.81(18)\times10^{-1}$
9.99×10^{-1}	$1.927(46)\times10^{-1}$
1.25×10^{0}	$1.572(38)\times10^{-1}$
2.50×10^{0}	$8.17(16)\times10^{-2}$
5.00×10^{0}	$3.34(20)\times10^{-2}$
1.25×10^{1}	$5.91(37)\times10^{-3}$
2.50×10^{1}	$9.19(38)\times10^{-4}$
5.00×10^{1}	$7.42(27)\times10^{-5}$
1.00×10^{2}	$2.74(13)\times10^{-6}$
2.00×10^{2}	$2.94(11)\times10^{-8}$
5.00×10^{2}	$9.48(44)\times10^{-12}$
1.00×10^{3}	$2.527(61)\times10^{-15}$
2.00×10^{3}	$5.16(24)\times10^{-20}$
5.00×10^{3}	$1.531(57)\times10^{-28}$
1.00×10^{4}	$2.90(50)\times10^{-37}$

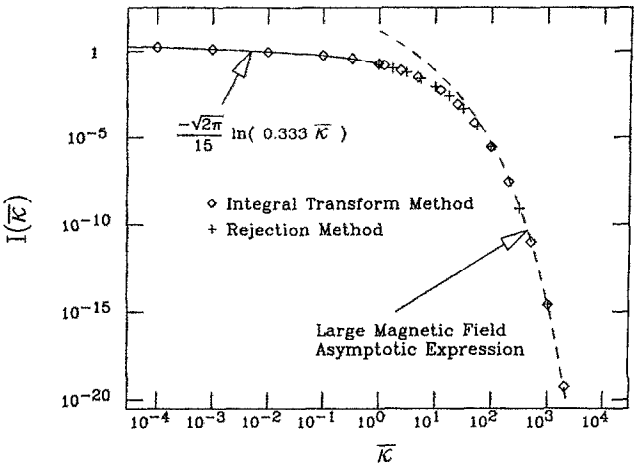

FIG. 1. Monte Carlo evaluation of the integral $I(\bar{\kappa})$ defined in Eq. (20). The evaluation via the integral transform method is shown as diamonds ($\diamond$) and via the rejection method is shown as crosses (+). The statistical uncertainty in the evaluation of the integral is approximately 5%. These results match on to the asymptotic formula of Ref. 3 (solid line) at small $\bar{\kappa}$ and onto Eq. (2) (dashed line) at large $\bar{\kappa}$.

minimum separation between the particles, the change in perpendicular energy $\Delta(u_1^2/2)$ can be calculated by integration along unperturbed orbits, and the unperturbed orbits are nearly straight lines. Under this circumstance the distance r_m is very nearly the impact parameter as defined for a collision in an unmagnetized plasma. The contribution of these collisions to the integral expression for $I(\bar{\kappa})$ is $(\sqrt{2\pi}/15)\int dr_m/r_m$, which is logarithmically divergent. In our numerical treatment the divergence is cut off at the upper end (i.e., $r_m \sim r_c$) by dynamical shielding and at the lower end (i.e., $r_m \sim \bar{b}$) by the repulsion of like charges. In terms of the two approximations, unperturbed orbits and straight line orbits, the first fails at the lower end and the second at the upper end. The previous work[3] is based on integration along unperturbed orbits taking into account the magnetic field, so the upper cutoff arises naturally but the lower cutoff must be imposed in an *ad hoc* manner. The imposition of either cutoff in an *ad hoc* manner introduces an uncertainty in the argument of the logarithm, that is, the factor C is not determined. In our numerical treatment, the dynamics automatically provides both cutoffs, so the constant C is determined. The value $C = 0.333(65)$ is obtained by matching

TABLE II. Results of Monte Carlo calculation using the rejection method. Statistical error in the last two significant figures is shown in parentheses.

$\bar{\kappa}$	$I(\bar{\kappa})$
1.00×10^{0}	$1.74(13)\times10^{-1}$
1.78×10^{0}	$1.070(65)\times10^{-1}$
3.16×10^{0}	$6.34(47)\times10^{-2}$
5.62×10^{0}	$2.90(22)\times10^{-2}$
1.00×10^{1}	$9.54(75)\times10^{-3}$
1.78×10^{1}	$2.70(19)\times10^{-3}$
3.16×10^{1}	$4.58(36)\times10^{-4}$
5.62×10^{1}	$4.73(36)\times10^{-5}$
1.00×10^{2}	$2.75(16)\times10^{-6}$
3.16×10^{2}	$7.98(38)\times10^{-10}$
1.00×10^{3}	$2.56(19)\times10^{-15}$

$-\sqrt{2\pi}/15\ln(\bar{\kappa}C)$ to the numerical results for $\bar{\kappa}\leqslant10^{-2}$. This fit curve is then found to agree with the Monte Carlo results to within statistical error over an even larger range, $\bar{\kappa}\leqslant1$.

The numerical results match onto both asymptotic results quite well. From Fig. 1, one can see that the numerical results track the logarithmic dependence for $\bar{\kappa}\ll1$ and fall off exponentially in accord with the asymptotic formula for $\bar{\kappa}\gg1$. To make a more detailed comparison of the numerical results and the large $\bar{\kappa}$ asymptotic formula, we factor out the exponential dependence and plot $I(\bar{\kappa})\exp[5(3\pi\bar{\kappa})^{2/5}/6]$ vs $\bar{\kappa}$. In Fig. 2, the points are numerical results, the solid curve is the new asymptotic formula given in Eq. (2), and the dashed curve is the previous asymptotic formula.[1] One can see that the new formula is in much better agreement with the numerical results.

Figure 3 shows a comparison of our numerical results to measured values of the equipartition rate. The solid curve is an interpolation of the Monte Carlo values for $I(\bar{\kappa})$, and the dashed curve is an extrapolation using the asymptotic formula $I(\bar{\kappa}) = -(\sqrt{2\pi}/15)\ln[(0.333)\bar{\kappa}]$. The points are experimental values for $\nu/n\bar{v}\bar{b}^2$, which according to theory should equal $I(\bar{\kappa})$. The squares, crosses, and diamonds are results obtained by Beck *et al.*[4] on a magnetically confined pure electron plasma that is cooled to the cryogenic temperature range by cyclotron radiation. The rate was measured for three magnetic field strengths (30, 40, and 60 kG corresponding to the squares, crosses, and diamonds, respectively) and for a series of temperatures ranging from 30 to 10^4 K; this corresponds to a range of $\bar{\kappa}$ values from 10^{-2} to 10^2. The electron density was near $n = 8\times10^8/\text{cm}^3$. There is quite good overall agreement between the theory and the experiment; the discrepancy between the measured values and the theory at large $\bar{\kappa}$ may be due to a 30% systematic error in the

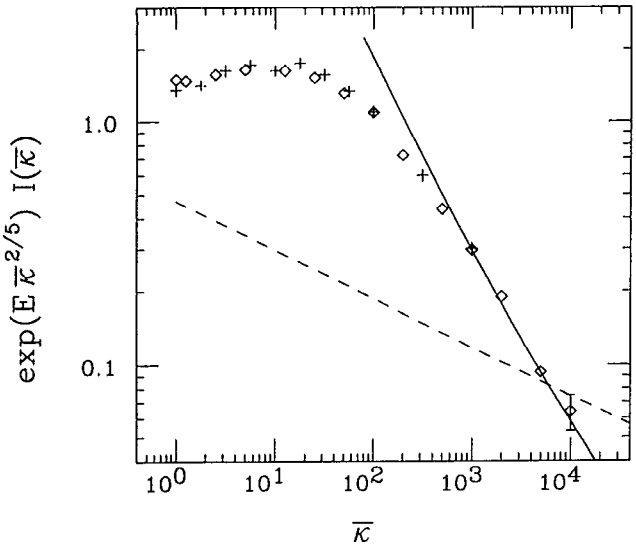

FIG. 2. Monte Carlo evaluation of $I(\bar{\kappa})$ for large $\bar{\kappa}$. The constant in the exponential factor multiplying the ordinate is $E = (5/6)(3\pi)^{2/5}$. The integral transform method results are shown as diamonds ($\diamondsuit$) and the rejection method results are shown as crosses (+). The statistical uncertainty is approximately 5% (the size of the symbols) unless otherwise indicated. The solid line is a plot of the new asymptotic formula Eq. (2) and the dashed line a plot of the previous asymptotic prediction of Ref. 1.

temperature measurement. Such an error is large enough to account for the discrepancy and would not be unreasonable for the diagnostic procedure used. Finally, the circles are results obtained by Hyatt *et al.*[5] from a closely related set of experiments also done with a magnetically confined pure electron plasma, but in an apparatus that is at room temperature with a magnetic field of 280 G. The full data set, enlarged by the room temperature experimental data, allows us to compare theory and experiment over a range of eight decades in $\bar{\kappa}$.

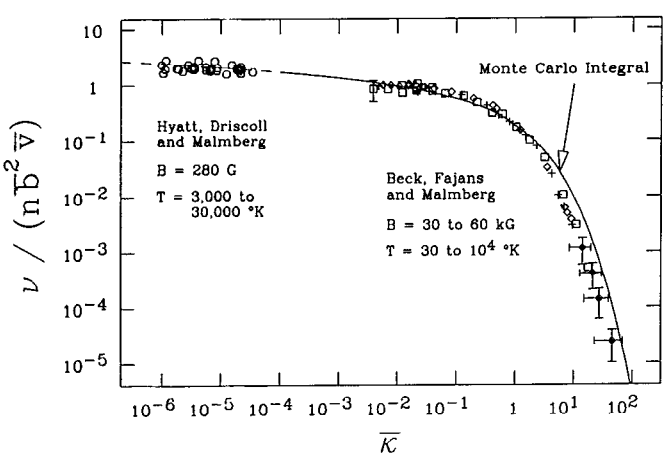

FIG. 3. Experimental results compared to the Monte Carlo evaluation of $I(\bar{\kappa})$. Shown are two sets of experiments. The first is the cryogenic experiment of Ref. 4. The experiment was conducted at three values of the magnetic field (+ = 30 kG, □ = 40 kG, and ◇ = 60 kG). The second is the room temperature experiment of Ref. 5, displayed as circles (○). The solid curve is an interpolation of the results of Table I. The dashed curve is an extrapolation using the formula $-(\sqrt{2\pi}/15)\ln[(0.333)\bar{\kappa}]$.

IV. ASYMPTOTIC EXPRESSION FOR THE EQUIPARTITION RATE IN THE LIMIT $\bar{\kappa} \gg 1$

In this section, we obtain the improved asymptotic formula for $I(\bar{\kappa})$ in the large $\bar{\kappa}$ limit that was written down in Eq. (2). As was mentioned earlier, the exponential dependence is the same as was obtained previously,[1] but the algebraic factor is different and more accurate; it is correct to higher order as an asymptotic expansion based on the smallness of $1/\bar{\kappa}$. The second and fourth terms in the expansion enter with surprisingly large numerical coefficients, and the first term does not dominate until $\bar{\kappa} > 10^5$, which is beyond the largest value of $\bar{\kappa}$ considered in the numerical calculations. It is necessary to retain the higher-order terms to obtain good agreement with the numerical results. We believe that the numerical coefficients in the expansion are reasonably accurate, but further refinement of the calculation would lead to some modification of these coefficients.

The first step is to obtain a more accurate asymptotic result for the energy exchange $\Delta E_\perp$. To this end we rewrite Eq. (12) for the relative motion in Hamiltonian form by using

$$H(r,p_r;z,p_z;\theta,p_\theta) = \frac{[p_\theta - (\mu\Omega_c/2)r^2]^2}{2\mu r^2} + \frac{p_r^2}{2\mu} + \frac{p_z^2}{2\mu} + \frac{e^2}{\sqrt{r^2+z^2}}, \tag{28}$$

where (r,θ,z) are cylindrical coordinates and (p_r,p_θ,p_z) are the conjugate momenta. Since θ is cyclic, p_θ is a constant of the motion. We can reduce the degrees of freedom to two and write the Hamiltonian as

$$H(r,p_r;z,p_z) = (p_r^2/2\mu) + (p_z^2/2\mu) + V(r,z), \tag{29}$$

where

$$V(r,z) \equiv \frac{\mu\Omega_c^2}{8}\left(r^2 - 2r_0^2 + \frac{r_0^4}{r^2}\right) + \frac{e^2}{\sqrt{r^2+z^2}} \tag{30}$$

and $r_0 \equiv \sqrt{2p_\theta/(\mu\Omega_c)}$. It is useful to approximate $V(r,z)$ as a harmonic potential in r at constant z by Taylor expanding; this gives

$$V(r,z) \approx V_g(z) + [\mu\Omega^2(z)/2][r - r_g(z)]^2, \tag{31}$$

where

$$\left.\frac{\partial V}{\partial r}\right|_{r=r_g} = 0, \quad V_g(z) = V[r_g(z),z]$$

and

$$\Omega^2(z) = \frac{1}{\mu}\left.\frac{\partial^2 V}{\partial r^2}\right|_{r=r_g}.$$

As z goes to infinity $\Omega(z)$ approaches Ω_c and $r_g(z)$ approaches r_0. One can identify $r_g(z)$ as the guiding center, $V_g(z)$ as the potential at the guiding center and $\Omega(z)$ as the effective cyclotron frequency.

We have neglected terms in the Taylor expansion of $V(r,z)$ that are of higher than quadratic order in $(r - r_g)$. It is found in the Appendix that the cubic term in the Taylor expansion contributes to terms of order $\bar{\kappa}^{-17/15}$. These terms are not significant when the asymptotic expression is compared to the numerical results.

It is useful to change independent variables from t to z. This is effected by using Hamilton's principle[13]

$$O = \delta \int_{t_1}^{t_2} \left(p_r \frac{dr}{dt} + p_z \frac{dz}{dt} - H \right) dt$$

$$= \delta \int_{z_1}^{z_2} \left(p_r \frac{dr}{dz} - H \frac{dt}{dz} + p_z \right) dz. \tag{32}$$

One can identify the new Hamiltonian as

$$H'(r,p_r;z) = -p_z = \mp \sqrt{2\mu \left(H - V_g(z) - \frac{\mu \Omega^2(z)}{2} [r - r_g(z)]^2 - \frac{p_r^2}{2\mu} \right)}, \tag{33}$$

where (r,p_r) and $(t, -H)$ are canonically conjugate coordinates and momenta. Since there is no explicit t dependence in H', the momentum H is a constant of the motion.

By using the generating function

$$S(P,r;z) = \int_{r'=r_g}^{r} \mu\Omega \sqrt{\frac{2}{\mu\Omega} P - (r' - r_g)^2}\, dr', \tag{34}$$

we introduce the action angle variables

$$P = \frac{1}{2\pi} \oint p_r\, dr = \frac{H - V_g - (p_z^2/2\mu)}{\Omega} \tag{35a}$$

and

$$\psi = \sin^{-1} \left[\sqrt{(\mu\Omega/2P)} (r - r_g) \right], \tag{35b}$$

and obtain the new Hamiltonian $H'' = -p_z + \partial S/\partial z|_{r,P}$. The generating function can be rewritten as

$$S(\psi,P) = P \sin\psi \cos\psi + P\psi, \tag{36}$$

so the needed partial derivative is given by

$$\left. \frac{\partial S}{\partial z} \right|_{r,P} = 2P \cos^2\psi \left. \frac{\partial \psi}{\partial z} \right|_{r,P}, \tag{37}$$

where $\partial\psi/\partial z|_{r,P} \cos\psi$ is easily evaluated from $\sin\psi = \sqrt{\mu\Omega/2P}\,(r - r_g)$. The new Hamiltonian is then

$$H''(P,\psi;z) = \mp \sqrt{2\mu(H - V_g - \Omega P)} - \sqrt{2\mu\Omega P} \frac{dr_g}{dz} \times \cos\psi + \frac{P}{2} \sin 2\psi \frac{d}{dz} (\ln \Omega). \tag{38}$$

We need to solve Hamilton's equations

$$\frac{dP}{dz} = -\sqrt{2\mu\Omega P} \frac{dr_g}{dz} \sin\psi - P \cos 2\psi \frac{d(\ln\Omega)}{dz}, \tag{39a}$$

$$\frac{d\psi}{dz} = \mp \frac{\mu\Omega}{\sqrt{2\mu(H - V_g - \Omega P)}} - \sqrt{\frac{\mu\Omega}{2P}} \frac{dr_g}{dz} \cos\psi + \left(\frac{1}{2} \right) \sin 2\psi \frac{d(\ln\Omega)}{dz}, \tag{39b}$$

in order to obtain the energy exchange $\Delta E_\perp = \Omega_c \Delta P$, and to this end we introduce a perturbative expansion

$$P = P^{(0)} + P^{(1)} + \cdots$$

and

$$\psi = \psi^{(0)} + \psi^{(1)} + \cdots.$$

The expansion parameter is r_*/z, where $r_*^3 = 4mc^2/B^2 = 2r_c^2 \bar{b}$. During the collision, the expansion parameter gets no larger than $r_*/b = (v_{\|0}/\Omega_c b)^{2/3} \ll 1$, where $b \equiv e^2/(\mu v_{\|0}^2/2)$. However, we will deform the z contour used to evaluate $\Delta E_\perp$ from the true trajectory to one which encircles the branch point of the integrand. On the deformed contour, r_*/z will be of order unity. Although the contribution of higher order $\Delta P^{(j)}$ will not be algebraically smaller, they will be numerically smaller. We refer one to the Appendix where we show that $\Delta P^{(j)} \sim 1/(\frac{2}{3}j - \frac{2}{3})!$

Turning our attention to finding the equations for $P^{(j)}$ and $\psi^{(j)}$, we first note that dr_g/dz and $d\Omega/dz$ are both of fourth order in the expansion parameter. This implies, in conjunction with Eqs. (39), that $dP^{(j)}/dz = 0$ and $d\psi^{(j)}/dz = 0$ if $j \neq 0,4,8,\ldots$. In addition one can see that $dP^{(0)}/dz = 0$,

$$\frac{dP^{(4)}}{dz} = -\sqrt{2\mu\Omega P^{(0)}} \frac{dr_g}{dz} \sin\psi^{(0)} - P^{(0)} \cos 2\psi^{(0)} \frac{d(\ln\Omega)}{dz}, \tag{40a}$$

and

$$\frac{d\psi^{(0)}}{dz} = \mp \frac{\mu\Omega}{\sqrt{2\mu(H - V_g - \Omega P^{(0)})}}. \tag{40b}$$

Since $dP^{(0)}/dz = 0$, we can set $P^{(0)} = P_0$, the precollision value. We will want to integrate Eq. (40a) to find $\Delta P^{(4)}$. The first term on the right-hand side of Eq. (40a) gives a contribution to $\Delta P^{(4)}$ of the form of an integral of $e^{i\psi^{(0)}}$ times a slowly varying function of $\psi^{(0)}$. The second term gives an integral of $e^{i2\psi^{(0)}}$ times a slowly varying function of $\psi^{(0)}$. This is an exponentially smaller contribution to $\Delta P^{(4)}$ compared to the first term. Hence we drop the second term on the right-hand side and write

$$\frac{dP^{(4)}}{dz} = -\sqrt{2\mu\Omega P_0} \frac{dr_g}{dz} \sin\psi^{(0)}, \tag{41a}$$

and

$$\frac{d\psi^{(0)}}{dz} = \mp \frac{\mu\Omega}{\sqrt{2\mu(H - V_g - \Omega P_0)}}. \tag{41b}$$

Since $\Delta P^{(0)} = 0$ over the course of a collision, we let $\Delta P \approx \Delta P^{(4)}$ with an estimated error of order $\Delta P^{(8)}/\Delta P^{(4)} \sim 2!/(14/3)! \approx 10^{-2}$. Integration of Eq. (41b) gives

$$\psi^{(0)} = \psi_0 + \alpha \mp \beta(z), \tag{42}$$

where ψ_0 is the initial gyroangle, α is the constant

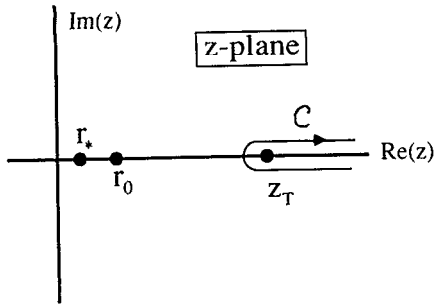

FIG. 4. Contour in the z plane used to find $\Delta E_\perp$. Here, z_T is the turning point where $p_z = 0$.

$$\alpha \equiv \pm \int_{z_T}^{z_0} \frac{\mu\Omega\, dz}{\sqrt{2\mu(H - V_g - \Omega P_0)}}, \tag{43}$$

z_T is the turning point where $H = V_g(z_T) + P_0\Omega(z_T)$, and

$$\beta(z) \equiv \int_{z_T}^{z} \frac{\mu\Omega(z')dz'}{\sqrt{2\mu[H - V_g(z') - P_0\Omega(z')]}}. \tag{44}$$

Substitution of the expression for $\psi^{(0)}$ given in Eq. (42) into Eq. (41a) and integration along the contour shown in Fig. 4 gives

$$\Delta^2 E_\perp \approx \Omega_c^2 \Delta^2 P^{(4)} = 4P_0\Omega_c^2 D\cos^2(\psi_0 + \alpha), \tag{45}$$

where

$$D \equiv \left| \int_C e^{i\beta(z)} \sqrt{\frac{\mu\Omega(z)}{2}} \frac{dr_g(z)}{dz}\, dz \right|^2. \tag{46}$$

The character of contour integral (46) is what one normally encounters when dealing with the breaking of adiabatic invariants.[14] When evaluated along the curve in Fig. 4 (i.e., along the true z trajectory), the integrand consists of a slowly varying factor $\sqrt{\Omega}\, dr_g/dz$ times a rapid oscillating factor $e^{i\beta}$. To evaluate such an integral, one deforms the contour into the complex plane so that the rapid oscillating factor becomes exponentially small. This continuation is extended until a singularity of the integrand is encountered, as shown in Fig. 5. For our case, the scale length for this singularity is the larger of r_* and r_0. One can identify these as the germaine length scales by determining on what length scale the two terms on the right-hand side of Eq. (30), the expression for $V(r,z)$, are of the same order of magnitude.

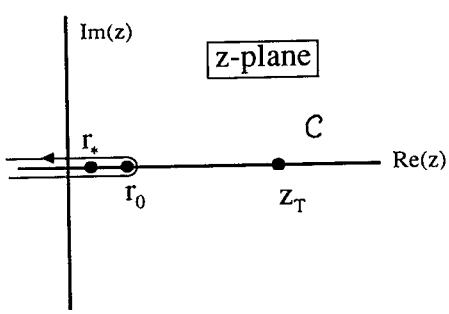

FIG. 5. Deformation of contour in the z plane used to find $\Delta E_\perp$.

In the Appendix we find $\beta(z)$ as a power series expansion in $(v_{\|0}/\Omega_c b)^{2/3}$ and $(v_{\perp 0}/v_{\|0})^2$ whose coefficients are functions of r_0/r_*. Since both $v_{\|0}/\Omega_c b \ll 1$ and $v_{\perp 0}/v_{\|0} \ll 1$ when the integrand in Eq. (20) gives a significant contribution to $I(\bar{\kappa} \gg 1)$, we can expand $e^{i\beta}$ in a power series. This series is substituted into Eq. (46), the contour integral done, and the result squared to obtain $\Delta^2 E_\perp$. We then substitute the power series for $\Delta^2 E_\perp$ into Eq. (20) and do the integrals to obtain the asymptotic expression shown in Eq. (2).

ACKNOWLEDGMENTS

This work was supported by National Science Foundation Grant No. PHY87-06358, U.S. Department of Energy Grant No. DEFG03-88ER53275, the San Diego Supercomputer Center, and a National Science Foundation Graduate Fellowship.

APPENDIX: EVALUATION OF THE INTEGRALS IN THE ASYMPTOTIC EXPRESSION FOR $I(\bar{\kappa})$

To evaluate the expression for $\Delta E_\perp$ found in Eq. (45), it is convenient to introduce the variables $\zeta \equiv (v_{\perp 0}/v_{\|0})^2$, $\epsilon \equiv (\Omega_c b/v_{\|0})^{-2/3}$, $\gamma \equiv (r_0/r_*)^{3/2}$, and $t \equiv (z/r_*)$, where $b \equiv 2e^2/\mu v_{\|0}^2$ and $r_*^3 \equiv 8\mu c^2/B^2$. We also define the functions

$$f(\gamma;\tilde{t}) \equiv r_g/r_0, \tag{A1}$$

$$h(\gamma;\tilde{t}) \equiv (\Omega/\Omega_c)^2, \tag{A2}$$

$$g(\gamma;\tilde{t}) \equiv \epsilon t(V_g/(\mu v_{\|0}^2/2)), \tag{A3}$$

and

$$\bar{g}(\gamma,\zeta;\tilde{t}) \equiv g(\gamma;\tilde{t})/\{1 + \zeta[1 - h^{1/2}(\gamma;\tilde{t})]\}. \tag{A4}$$

The functions can all be expressed as convergent power series in $\tilde{t} \equiv 1/t$ for $t \gg \max(1,\gamma^{2/3})$. Equation (46) can now be rewritten as

$$D = \frac{\mu\Omega_c r_0^2}{2} \left| \int_C \exp[i\beta(\epsilon,\gamma,\zeta;\tilde{t})] \times h^{1/4}(\gamma;\tilde{t}) \frac{df(\gamma;\tilde{t})}{dt}\, dt \right|^2, \tag{A5}$$

where

$$i\beta(\epsilon,\gamma,\zeta;\tilde{t}) = \int_{t' = t_T}^{t} \frac{h^{1/2}(\gamma;\tilde{t}')g^{-1/2}(\gamma;\tilde{t}')(t')^{1/2}\, dt'}{\sqrt{1 - \epsilon t'\bar{g}^{-1}(\gamma,\zeta;t')}}, \tag{A6}$$

$\bar{g}(\gamma,\zeta;\tilde{t}_T) = \epsilon t_T$, and the contour C is shown in Fig. 6.

Let us first work on the evaluation of integral in the definition of $i\beta$. Make the change of variable from t to s defined by

$$s \equiv \epsilon t\bar{g}^{-1}(\gamma,\zeta;\tilde{t}). \tag{A7}$$

The function $\bar{g}^*$ is defined to be the inverse of $\bar{g}$, that is,

$$\tilde{s} = \tilde{t}\bar{g}(\gamma,\zeta;\tilde{t}) \tag{A8}$$

is equivalent to

$$\tilde{t} = \tilde{s}\bar{g}^*(\gamma,\zeta;\tilde{s}), \tag{A9}$$

where $\tilde{s} \equiv \epsilon/s$. Since we can expand $\bar{g}$ in a convergent power series in $\tilde{t}$, we can do a series inversion to find the power series for $\bar{g}^*$. This allows us to write Eq. (A6) in the form

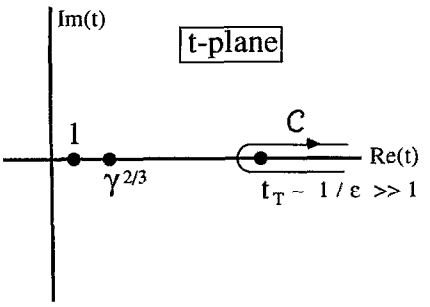

FIG. 6. Contour in the t plane used to find D. The parameter t_T is of order $1/\epsilon$ which is much greater than 1 for large values of the magnetic field.

$$i\beta = -\epsilon^{-3/2}\int_{s=\delta}^{1}\left(\frac{h[\gamma;\bar{s}\bar{g}^*(\gamma,\zeta;\tilde{s})]}{1+\zeta\{1-h^{1/2}[\gamma;\bar{s}\bar{g}^*(\gamma,\zeta;\tilde{s})]\}}\right)^{1/2} \times[\bar{g}^*(\gamma,\zeta;\tilde{s})]^{-2}\left(\bar{g}^*(\gamma,\zeta;\tilde{s})+\tilde{s}\frac{d\bar{g}^*(\gamma,\zeta;\tilde{s})}{d\tilde{s}}\right) \times\frac{s^{1/2}\,ds}{\sqrt{1-s}}, \tag{A10}$$

where $\delta\equiv\epsilon\bar{t}\bar{g}^{-1}(\gamma,\zeta;\tilde{t})$. The part of the integrand written as a function of $\tilde{s}$ can be expanded into a power series in $\tilde{s}$ with the expansion coefficients $a_n(\gamma,\zeta)$. Substituting this power series into Eq. (A10) and exchanging the summation and integration gives us

$$i\beta = -\epsilon^{-3/2}\sum_{n=0}^{\infty}a_n(\gamma,\zeta)\epsilon^n\int_{s=\delta}^{1}\frac{s^{1/2-n}\,ds}{\sqrt{1-s}}. \tag{A11}$$

The integral can be done by changing the variable of integration to $u\equiv(1-s)/(1-\delta)$ and applying the integral representation of the hypergeometric function[15]

$$ {}_2F_1(a,b;c;z) = \frac{\Gamma(c)}{\Gamma(b)\Gamma(c-b)}\int_0^1 s^{b-1}(1-s)^{c-b-1}(1-zs)^{-a}\,ds, \tag{A12}$$

leaving us with

$$i\beta = -\epsilon^{-3/2}\sum_{n=0}^{\infty}a_n(\gamma,\zeta)\epsilon^n 2(1-\delta)^{1/2} \times{}_2F_1\left(-\frac{1}{2}+n,\frac{1}{2};\frac{3}{2};1-\delta\right). \tag{A13}$$

Application of the linear transformation formula[15]

$$ {}_2F_1(a,b;c;z) = \frac{\Gamma(c)\Gamma(c-a-b)}{\Gamma(c-a)\Gamma(c-b)}{}_2F_1(a,b;a+b-c+1;1-z) + (1-z)^{c-a-b}\frac{\Gamma(c)\Gamma(a+b-c)}{\Gamma(a)\Gamma(b)} \times{}_2F_1(c-a,c-b;c-a-b+1;1-z), \tag{A14}$$

and use of the fact that $a_0=1$ and $a_1=0$, yields

$$i\beta = -\frac{\pi\kappa}{2}-\sum_{n=0}^{\infty}a_n(\gamma,\zeta)\epsilon^{n-3/2}\delta^{3/2-n}(1-\delta)^{1/2} \times\frac{2}{2n-3}{}_2F_1\left(2-n,1;\frac{5}{2}-n;\delta\right), \tag{A15}$$

where $\kappa\equiv\epsilon^{-3/2}$. Expanding $(1-\delta)^{1/2}{}_2F_1(2-n,1;\frac{5}{2}-n;\delta)$ in a power series in δ and substituting $\delta=\epsilon\bar{t}\bar{g}^{-1}$ gives

$$i\beta = -\frac{\pi\kappa}{2}-\sum_{k=0}^{\infty}\epsilon^k t^{k+3/2}\sum_{n=0}^{\infty}a_n(\gamma,\zeta)b_{nk}\tilde{t}^{\,n} \times[\bar{g}(\gamma,\zeta;\tilde{t})]^{n-k-3/2}, \tag{A16}$$

where

$$b_{nk}\equiv\frac{2}{2n-3}\sum_{m=0}^{k}\frac{(2-n)_{k-m}(-\frac{1}{2})_m}{(\frac{5}{2}-n)_{k-m}m!}. \tag{A17}$$

As a last step, expand $(\bar{g})^{n-k-3/2}$ in a power series such that

$$[\bar{g}(\gamma,\zeta;\tilde{t})]^{j-3/2} = \sum_{i=0}^{\infty}c_{ji}(\gamma,\zeta)\tilde{t}^{\,i} \tag{A18}$$

and define

$$F_k(\gamma,\zeta;\tilde{t})\equiv-\sum_{i=0}^{\infty}d_{ki}(\gamma,\zeta)\tilde{t}^{\,i}, \tag{A19}$$

where

$$d_{ki}(\gamma,\zeta)\equiv\sum_{n=0}^{i}a_n(\gamma,\zeta)b_{nk}c_{n-k,i-n}(\gamma,\zeta). \tag{A20}$$

One can further reduce F_k to the form

$$F_k(\gamma,\zeta;\tilde{t}) = \sum_{l=0}^{k}F_{kl}(\gamma;\tilde{t})\left(\frac{\zeta}{t^3}\right)^l \tag{A21}$$

because of the structure of $d_{ki}(\gamma,\zeta)$. The structure was found by use of the symbolic algebra package MATHEMATICA[16] for $k=0,\ldots,4$. Since we only use $k=0,1,2$ terms, such a reduction in F_k is justified for our purposes. This gives us the final form for $i\beta$, namely

$$i\beta = -\frac{\pi\kappa}{2}+\sum_{k=0}^{\infty}\sum_{l=0}^{k}\epsilon^k\zeta^l t^{k-3l+3/2}F_{kl}(\gamma;\tilde{t}). \tag{A22}$$

Now substitute $i\beta$ into Eq. (A5) to obtain

$$D = (\mu\Omega_c r_0^2/2)e^{-\pi\kappa}|J(\epsilon,\zeta;\gamma)|^2, \tag{A23}$$

where we have defined

$$J(\epsilon,\zeta;\gamma)\equiv\int_C\exp\left(\sum_{k=0}^{\infty}\sum_{l=0}^{k}\epsilon^k\zeta^l t^{k-3l+3/2}F_{kl}(\gamma;\tilde{t})\right) \times h^{1/4}(\gamma;\tilde{t})\frac{df(\gamma;\tilde{t})}{dt}\,dt. \tag{A24}$$

For large values of the magnetic field, we will only need to know J where $\epsilon,\zeta\ll1$. Therefore, we can expand the exponential to give

$$J(\epsilon,\zeta;\gamma) = \sum_{k=0}^{\infty}\sum_{l=0}^{k}\epsilon^k\zeta^l B_{kl}(\gamma), \tag{A25}$$

where

$$B_{kl}(\gamma)\equiv\int_C G_{kl}(\gamma;\tilde{t})\exp[t^{3/2}F_{00}(\gamma;\tilde{t})] \times h^{1/4}(\gamma;\tilde{t})\frac{df(\gamma;\tilde{t})}{dt}\,dt \tag{A26}$$

and

$$G_{00}(\gamma;\tilde{t})\equiv1, \tag{A27a}$$

$$G_{10}(\gamma;\tilde{t})\equiv t^{5/2}F_{10}(\gamma;\tilde{t}), \tag{A27b}$$

$$G_{20}(\gamma;\tilde{t})\equiv t^{7/2}F_{20}(\gamma;\tilde{t})+\tfrac{1}{2}t^5F_{10}^2(\gamma;\tilde{t}), \tag{A27c}$$

$$G_{11}(\gamma;\tilde{t}) \equiv t^{-1/2} F_{11}(\gamma;\tilde{t}), \tag{A27d}$$

etc. This will allow us to write

$$\gamma^2 |J(\epsilon,\zeta;\gamma)|^2 = \sum_{k=0}^{\infty} \sum_{l=0}^{k} \epsilon^k \zeta^l A_{kl}(\gamma), \tag{A28}$$

where

$$A_{00}(\gamma) \equiv B_{00}^2(\gamma)\gamma^2, \tag{A29a}$$

$$A_{10}(\gamma) \equiv 2B_{10}(\gamma)B_{00}(\gamma)\gamma^2, \tag{A29b}$$

$$A_{20}(\gamma) \equiv [2B_{20}(\gamma)B_{00}(\gamma) + B_{10}^2(\gamma)]\gamma^2, \tag{A29c}$$

$$A_{11}(\gamma) \equiv 2B_{11}(\gamma)B_{00}(\gamma)\gamma^2, \tag{A29d}$$

etc. Finally we can write the change in the perpendicular energy as

$$\Delta^2 E_\perp = (\mu v_{10}^2)\left(\frac{2e^2}{r_0}\right)\cos^2(\psi_0 + \alpha) e^{-\pi\kappa} \sum_{k=0}^{\infty} \sum_{l=0}^{k} \epsilon^k \zeta^l A_{kl}(\gamma). \tag{A30}$$

We substitute this expression into Eq. (20) to obtain

$$I(\bar{\kappa}) = \frac{1}{9\sqrt{2\pi}} \sum_{k=0}^{\infty} \sum_{l=0}^{k} \left(\int_0^\infty \frac{d\gamma}{\gamma^{1/3}} A_{kl}(\gamma)\right) \times \left(\int_0^\infty u_1^{2l+3} e^{-u_1^2/2}\, du_\perp\right)\left(\int_0^{2\pi} d\psi \cos^2(\psi+\alpha)\right) \times \left\{\bar{\kappa}^{-2l/3} \int_0^\infty d\kappa\, \kappa^{-5/3+(2/3)(l-k)} \times \exp\left[-\pi\kappa - \frac{1}{2}\left(\frac{\bar{\kappa}}{\kappa}\right)^{2/3}\right]\right\}. \tag{A31}$$

Defining $A_{kl} \equiv (\int_0^\infty d\gamma/\gamma^{1/3}) A_{kl}(\gamma)$ and doing the γ, $u_\perp$, and ψ integrals gives

$$I(\bar{\kappa}) = \frac{\sqrt{2\pi}}{9} \sum_{k=0}^{\infty} \sum_{l=0}^{k} A_{kl} 2^l \Gamma(l+2) \bar{\kappa}^{-2l/3} \times \left\{\int_0^\infty d\kappa\, \kappa^{-5/3+(2/3)(l-k)} \times \exp\left[-\pi\kappa - \frac{1}{2}\left(\frac{\bar{\kappa}}{\kappa}\right)^{2/3}\right]\right\}. \tag{A32}$$

Evaluation of the κ integral via the method of steepest descent as $\bar{\kappa} \to \infty$ leads us to the asymptotic series

$$I(\bar{\kappa}) \underset{\bar{\kappa}\to\infty}{\to} e^{-(5/6)(3\pi\bar{\kappa})^{2/5}} \frac{\sqrt{2\pi}}{9} \sum_{k=0}^{\infty} \sum_{l=0}^{k} \sum_{n=0}^{\infty} \times A_{kl} 2^l \Gamma(l+2)\Gamma\left(n+\frac{1}{2}\right) e_{2n}\left(\frac{5}{3} + \frac{2}{3}(k-l)\right) \times \bar{\kappa}^{-7/15 - (2/15)(2k+3l+3n)}, \tag{A33}$$

where

$$\omega^2 \equiv (\pi/x) + \tfrac{1}{2}x^{2/3} - \tfrac{5}{6}(3\pi)^{2/5} \tag{A34}$$

and

$$\frac{dx}{d\omega} x^{\beta-2} = \sum_{k=0}^{\infty} e_k(\beta)\omega^k. \tag{A35}$$

Keeping terms to order $\bar{\kappa}^{-19/15}$, one finds that

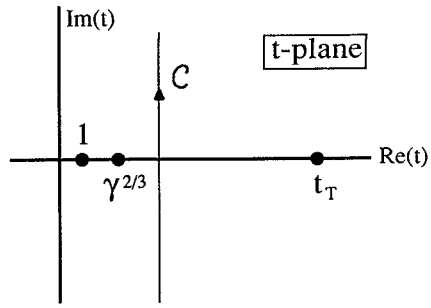

FIG. 7. Contour in the t plane used in the numerical contour integration of $B_{kl}(\gamma)$.

$$I(\bar{\kappa}) e^{(5/6)(3\pi\bar{\kappa})^{2/5}} \underset{\bar{\kappa}\to\infty}{\to} \frac{2\pi(3\pi)^{1/5}}{3\sqrt{5}} A_{00}\bar{\kappa}^{-7/15} + \frac{2\pi(3\pi)^{3/5}}{3\sqrt{5}} A_{10}\bar{\kappa}^{-11/15} + \frac{14(3\pi)^{4/5}}{135\sqrt{5}} A_{00}\bar{\kappa}^{-13/15} + \frac{2\pi^2}{\sqrt{5}} A_{20}\bar{\kappa}^{-15/15} + \frac{8(3\pi)^{6/5}}{135\sqrt{5}} (7A_{10} + 15A_{11})\bar{\kappa}^{-17/15} + O(\bar{\kappa}^{-19/15}). \tag{A36}$$

We have now reduced the problem to that of finding a numerical value for the A_{kl}. We do this by first finding the power series expansions for the functions f, h, and g to 30th order in $\tilde{t}$ with the help of the symbolic algebra package MATHEMATICA.[16] The large number of terms were needed to obtain accuracy in the A_{kl} of at least one part in 10^4. It is then a straightforward process to find power series expansions for the $F_{kl}(\gamma;\tilde{t})$, substitute them into the integral expressions for $B_{kl}(\gamma)$ given in Eq. (A26), and then to numerically evaluate the integrals along the contour shown in Fig. 7. We choose this particular deformation of the contour to reduce the oscillations of the factor $\exp[t^{3/2}F_{00}(\gamma;\tilde{t})]$ in the integrand. We cannot take the contour any closer to the origin than $\max(1,\gamma^{2/3})$ because of singularities in the integrand which are manifested by the series expansions no longer converging. Once the γ dependence of $B_{kl}(\gamma)$ is found by doing many numerical integrations of Eq. (A26), each for a different value of γ; we obtain a graph of $A_{kl}(\gamma)$ by the simple algebraic combination of the $B_{kl}(\gamma)$ given in Eqs. (A29). The results are shown in Fig. 8, which displays all the $A_{kl}(\gamma)$ needed to evaluate $I(\bar{\kappa})$ to $\bar{\kappa}^{-19/15}$ order. All four displayed functions have the same basic functional form: they peak at $\gamma \approx 1$, scale as γ^2 at small values of γ, and go to zero exponentially in γ at large values of γ. It is now a simple matter to numerically integrate these functions to find A_{kl}. When the results are substituted into Eq. (A36) we are left with the asymptotic formula for $I(\bar{\kappa})$ shown in Eq. (2).

We now turn our attention to an estimation of the error we are making by only calculating $\Delta P^{(4)}$. This is most easily seen by examining the expression for $B_{kl}(\gamma)$ given in Eq. (A26). Since the A_{kl} are just integrated algebraic combinations of the $B_{kl}(\gamma)$, this is sufficient to estimate the error of the A_{kl}. We start by noting that the integral for $B_{kl}(\gamma)$ is of the form

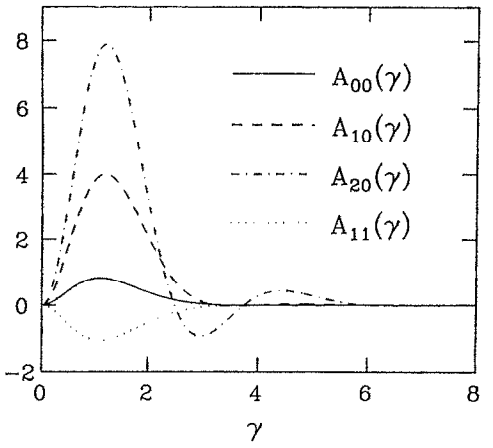

FIG. 8. The functions $A_{kl}(\gamma)$ which show the $\gamma=(r_0/r_*)^{3/2}$ dependence of $\Delta E_\perp$. See Eq. (A30) for the exact relationship between $A_{kl}(\gamma)$ and $\Delta E_\perp$.

$$B_{kl}(\gamma)\sim\int_C e^{t^{3/2}}t^{-4+n_{kl}}dt, \tag{A37}$$

where $G_{kl}(\gamma;\tilde{t})\sim\tilde{t}^{\,-n_{kl}}$ as $\tilde{t}\to 0$. The n_{kl} can easily be found by examination of the expressions for $G_{kl}(\gamma;\tilde{t})$ given in Eqs. (A27). One should remember that $F_{kl}(\gamma;\tilde{t})\sim 1$, $h(\gamma;\tilde{t})\sim 1$, and $df(\gamma;\tilde{t})/dt\sim\tilde{t}^{\,4}$ as $\tilde{t}\to 0$. This will aid one in finding the values of n_{kl} and the form of Eq. (A37). The fact that $df/dt\sim\tilde{t}^{\,4}$ is why the ΔP we are calculating is of fourth order; remember that $\tilde{t}=r_*/z$. The difference in the calculation of $B_{kl}^{(m)}(\gamma)$ which contributes to $\Delta P^{(m)}$ is the replacement of the "4" in Eq. (A37) with m. We can easily evaluate the integral on the right-hand side of Eq. (A37). Doing this we find that

$$B_{kl}^{(m)}(\gamma)\sim 1/\Gamma(2m/3-2n_{kl}/3+1/3). \tag{A38}$$

By using Eq. (A38), we can estimate that the coefficient of $\bar{\kappa}^{-7/15}$ in the asymptotic expression for $I(\bar{\kappa})$, Eq. (2), would be changed by about 1% by including the higher-order corrections to ΔP. The expected changes in all the coefficients are shown in the following expression of Eq. (2):

$$\begin{aligned} I(\bar{\kappa})e^{(5/6)(3\pi\bar{\kappa})^{2/5}} &\approx(1.83\pm 1\%)\bar{\kappa}^{-7/15}+(20.9\pm 10\%)\bar{\kappa}^{-11/15} \\ &\quad+(0.347\pm 1\%)\bar{\kappa}^{-13/15}+(87.8\pm 40\%)\bar{\kappa}^{-15/15} \\ &\quad+(6.68\pm 10\%)\bar{\kappa}^{-17/15}. \end{aligned} \tag{A39}$$

The other approximation we need to examine is neglecting the terms of order $(r-r_g)^3$ and higher in the Taylor expansion of $V(r,z)$, Eq. (30). One can see how these terms will effect the final result for $I(\bar{\kappa})$ by including the cubic term and repeating the calculation. When this is done one finds that $\Delta P^{(4)}$ is changed by an amount $\Delta(\Delta P^{(4)})$, which is smaller than $\Delta P^{(4)}$ by the ratio

$$\frac{\Delta(\Delta P^{(4)})}{\Delta P^{(4)}}\sim\frac{P_0}{m\Omega_c r_*^2}\sim\left(\frac{v_{10}/\Omega_c}{r_*}\right)^2\sim\epsilon\xi. \tag{A40}$$

Including this correction will modify A_{kl} with $k,l\geqslant 1$. Hence, keeping higher-order terms in the Taylor expansion will modify terms in the asymptotic expression for $I(\bar{\kappa})$ of order $\bar{\kappa}^{-17/15}$ or greater; terms which are small at the large values of $\bar{\kappa}$ of interest to us.

[1] T. M. O'Neil and P. G. Hjorth, Phys. Fluids **28**, 3241 (1985).
[2] S. Ichimaru and M. N. Rosenbluth, Phys. Fluids **13**, 2778 (1970).
[3] V. P. Silin, Sov. Phys. JETP **14**, 617 (1962); D. Montgomery, L. Turner, and G. Joyce, Phys. Fluids **17**, 954 (1974); D. Montgomery, G. Joyce, and L. Turner, *ibid.* **17**, 2201 (1974); G. Hübner and H. Schamel, Z. Naturforsch. **45a**, 1 (1990).
[4] B. R. Beck, J. Fajans, and J. H. Malmberg, Phys. Rev. Lett. **68**, 317 (1992).
[5] A. W. Hyatt, C. F. Driscoll, and J. H. Malmberg, Phys. Rev. Lett. **59**, 2975 (1987).
[6] T. M. O'Neil, Phys. Fluids **26**, 2128 (1983).
[7] E. M. Lifshitz and L. P. Pitaevskii, *Physical Kinetics* (Pergamon, Oxford, 1981), p. 168.
[8] N. Rostoker, Phys. Fluids **3**, 922 (1960).
[9] A. Lenard, Ann. Phys. (N.Y.) **10**, 390 (1960); R. Belescu, Phys. Fluids **3**, 52 (1960).
[10] I. M. Sobol, *The Monte Carlo Method* (MIR, Moscow, 1975).
[11] W. H. Press, B. P. Flannery, S. A. Tenkolsky, and W. T. Vetterling, *Numerical Recipes* (Cambridge U.P., Cambridge, 1986).
[12] P. G. Hjorth, Ph.D. thesis, University of California at San Diego, 1988; A. J. Lichtenberg and M. A. Lieberman, *Regular and Stochastic Motion* (Springer-Verlag, New York, 1983), p. 130.
[13] H. Goldstein, *Classical Mechanics* (Addison–Wesley, Reading, MA, 1980), p. 35.
[14] L. D. Landau and E. M. Lifshitz, *Mechanics* (Pergamon, Oxford, 1976), p. 157.
[15] M. Abramowitz and I. A. Stegun, *Handbook of Mathematical Functions* (Dover, New York, 1970).
[16] S. Wolfram, *Mathematica* (Addison–Wesley, Reading, MA, 1988).